Analysis and Application of Ligand Binding Mechanism of Receptor Proteins(Dissertation_全文)

AUTHOR(S):

Shimada, Yoshimi

Analysis and Application of

Ligand Binding Mechanism of Receptor Proteins

Yoshimi Shimada

2001

Analysis and Application of

Ligand Binding Mechanism of Receptor Proteins

Yoshimi Shimada

2001

CONTENTS

ABBREVIATIONS

BHK	baby hamster kidney
CAPS	*N*-cyclohexyl-3-aminopropanesulfonic acid
cDNA	complementary DNA
CRD	cysteine-rich domain
DTT	dithiothreitol
EGS	ethylene glycol bis(succinimidylsuccinate)
EIA	enzyme immunoassay
ELISA	enzyme-linked immunosorbent assay
GPCR	G-protein coupled receptor
Hepes	2-[4-(2-hydroxyethyl)-1-piperazinyl]ethanesulfonic acid
HRP	horseradish peroxidase
LBD	ligand binding domain
LIVBP	leucine-, isoleucine-, valine-binding protein
MAb	monoclonal antibody
mGluR	metabotropic glutamate receptor
PAGE	polyacrylamide gel electrophoresis
PCR	polymerase chain reaction
PEG	polyethylene glycol
PMSF	phenylmethylsulfonyl fluoride
RGD	arginyl-glycyl-aspartic acid
tPA	tissue-type plasminogen activator

INTRODUCTION

Proteins are involved in every aspect of life, playing crucial roles in all life processes, not only catalyzing biochemical reactions with remarkable specificity but also serving as essential elements in all cells and tissues. For example, membrane proteins regulate ion transport, intercellular recognition and communication. A subset of these are cell surface receptors and transduce an extracellular signal to intracellular proteins by drastically changing their structure upon binding ligand. Each receptor is specific for its ligand, which can be either insoluble such as adhesive proteins or extracellular matrices, or soluble, such as peptides or amino acids. Binding allosterically induces a structural change that is transmitted through the membrane to the intracellular portion of the receptor, which can then be recognized by the respective signalling pathway. All of these processes require receptor proteins to recognize ligands, and this recognition is encoded in the respective three dimensional structures of these proteins. Thus, to decipher the relationship between a protein's structure and its function is one of the central issues in protein science. Elucidating the detailed mechanism of molecular recognition reactions on a structural level is the key to design of useful proteins or ligands for therapeutic, diagnostic, industrial or technological applications. From this point of view, I studied the ligand binding mechanism of receptor proteins to reveal the structure-function relationship and to develop its application.

In CHAPTER I, I will describe the functional structure of the tripeptide Arg-Gly-Asp (RGD) sequence and its application. The RGD sequence was originally identified as the sequence within fibronectin (1) that mediates cell attachment. The RGD motif, now found in numerous other proteins (2, 3), mediates binding of these proteins to their receptors and often is involved in cell adhesion. Integrin, a family of

cell-surface proteins, act as receptors for cell adhesion molecules. A subset of these integrins recognize the RGD motif within their ligands, the binding of which mediates both cell-substratum and cell-cell interactions. An RGD peptide blocking the ligand binding region of the integrins can inhibit these interactions. RGD and mimetics, thus, are potential therapeutic agents for the treatment of diseases such as thrombosis and cancer, which are associated with aberrations in cell adhesion. Studies with synthetic RGD peptides have shown that the presence of charged side chains alone is not sufficient to confer binding activity. Computer-assisted modeling and NMR data suggested conformations with two β-bends of type III-III or III-I (4). Previously a series of structural studies of a function RGD sequence was done, by introducing it into human lysozyme of which the three-dimensional structure is already determined. It was figured out that type II' β-turn structure is essential to adhere cells through the interaction with the integrin receptors (5). SECTION I describes an application for the RGD-engineered human lysozyme molecule. This mutant with two site of introduced RGD sequence was produced with full lytic activity and divalent cell adhesive ability. These two sites are located at a considerable distance (19.4 Å). Thus the (47,74)RGD4 mutant may be useful as a functional cross-linker in RGD dependent cell-to-cell interactions. SECTION II contains the work involving engineering of the RGD sequence into tissue-type plasminogen activator (tPA), an essential component of the vascular thrombolytic system which converts plasminogen into plasmin, which in turn degrades fibrin clots and causes the dissolution of thrombi (6). To develop new therapeutic agents for thrombosis, I introduced the RGD sequence into tPA. With the high concentration of platelet in fibrin clots, I focused on platelet integrin $\alpha_{IIb}\beta_3$. I will show that an RGD-introduced tPA mutant possessed high affinity for the integrin $\alpha_{IIb}\beta_3$

as well as full tPA activity. This novel tPA would be targeted to the fibrin clots and useful as an improved thrombolytic agent for coronary thrombosis.

CHAPTER II describes the ligand binding region of metabotropic glutamate receptor subtype 1 (mGluR1), which is one of the neurotansmitter receptors involved in a variety of physical functions in the central nervous system including the modulation of synaptic transmission (7). In contrast to the classical G-protein coupled receptors (GPCRs), metabotropic glutamate receptors (mGluRs) contain large extracellular regions (~600 amino acids) (8). Previously the whole extracellular region of mGluR1 was expressed in a soluble form (9). In this chapter, I will describe the results of proteolytic analysis to elucidate domain organization and receptor-ligand binding of soluble extracellular region of mGluR1.

References

1. Pierschbacher, M. D., and Ruoslahti, E. (1984) *Nature* **309**, 30–33.
2. Suzuki, S., Oldberg, A., Hayman, E. G., Pierschbacher, M. D., and Ruoslahti, E. (1985) *EMBO J.* **4**, 2519–2524.
3. Watt, K. W. K., Cottrall, B. A., Strong, D. D., and Doolittle, R. F. (1979) *Biochemistry* **18**, 5410–5416.
4. Reed, J., Hull, W. E., von der Lieth, C.-W., Kübler, D., Suhai, S., and Kinzel V. (1988) *Eur. J. Biochem.* **178**, 141–154.
5. Yamada, T., Song, H., Inaka, K., Shimada, Y., Kikuchi, M., and Matsushima, M. (1995) *J. Biol. Chem.* **270**, 5687–5690.
6. Pennica, D., Holmes, W. E., Kohr, W. J., Harkins, R. N., Vehar, G. , Ward, G. A., Benett, W. F., Yelverton, E., Seeburg, P. H., Heyneker, H. L., Goeddel, D.

V., and Collen, D. (1983) *Nature* **301**, 214–221.

7. Masu, M., Tanabe, Y., Tsuchida, K., Shigemoto, R., and Nakanishi, S. (1991) *Nature* **349**, 760–765.

8. Nakanishi, S., and Masu, M. (1994) *Annu. Rev. Biophys. Biomol. Struct.* **23**, 319–348.

9. Okamoto, T., Sekiyama, N., Otsu, M., Shimada, Y., Sato, A., Nakanishi, S., and Jingami, H. (1998) *J. Biol. Chem.* **273**, 13089–13096.

CHAPTER I

Analysis and application of ligand binding mechanism of Arg-Gly-Asp sequence

SECTION I

Construction of a divalent cell adhesive lysozyme by introducing the Arg-Gly-Asp sequence at two sites

Introduction

The Arg-Gly-Asp (RGD) sequence is well-known as a site in cell adhesive protein such as fibronectin (1), vitronectin (2), and fibrinogen (3) for binding to their receptors, the integrin (4). Previously a mutant 74RGD4 was constructed by inserting RGDS of human fibronectin between ^{74}Val and ^{75}Asn in a flexible loop region of human lysozyme using a yeast expression system (5). To increase the cell adhesion activity of the 74RGD4 mutant, we constructed another mutant, Cys-RGD4, by inserting RGDS flanked by two Cys residues at the same site in the lysozyme molecules (6). This design is based on the fact that the cyclic form of an RGD-containing peptide has much higher affinity to the integrins than the linear counterpart (7). For both mutants, we have already reported the structural and functional analyses, and discussed the functional conformation of the RGD sequence (5, 8).

In parallel with the construction of Cys-RGD4, another design has been tried to tailor the 74RGD4 mutant to possess higher adhesion activity. In this study, one more RGD introduction site was searched for in the lysozyme molecule. Here I report the construction of (47,74)RGD4, a mutant lysozyme containing RGD at two sites, and its functional evaluation. The structural feature of the possible introduction site of RGD in human lysozyme is discussed, in connection with the functional conformation of RGD.

Materials and methods

Vector constructions

Oligonucleotides were chemically synthesized using an automated DNA synthesizer (Model 380B, Applied Biosystems). The mutation was performed in M13mp19XhLZM using the site-directed mutagenesis system Mutan-K (Takara Shuzo). The primer used for the construction of 47RGD4, for example, was 5'-AGTCTGTAGAACTGTCGCCACGGTTGTAATT-3'. The underlined bases indicate mismatches. The sequence of the mutated gene was confirmed by dideoxy sequencing. The genes encoding the signal sequence and the mutated human lysozyme were combined with an *Xho*I-*Sma*I large fragment from pERI8602 (9) to construct the expression plasmid.

The M13mp19XhLZM plasmid possesses an *Xba*I restriction site between codons corresponding to ^{61}Ser and ^{62}Arg of human lysozyme (9). To construct the (47,74)RGD4 expression plasmid, the following three fragments were combined: an *Xho*I-*Xba*I fragment encoding the signal sequence and the NH_2-terminal domain of 47RGD4, an *Xba*I-*Sma*I fragment encoding the COOH-terminal domain of 74RGD4 (5), and an *Xho*I-*Sma*I large fragment from pERI8602.

Expression and purification of mutant human lysozymes

Mutant human lysozymes were expressed in yeast as described previously (10). Secreted mutant lysozymes were purified essentially as described (9). HPLC was performed using a cation-exchange column (Asahipak ES-502C; Asahikasei, Japan) and hydroxyapatite column (TAPS-020810, Tonen K.K., Japan).

Measurement of activity

Lytic activity was measured using *Micrococcus lysodeikticus* cells as a substrate (9). Protein was determined by measuring the weight in the freeze-dried form of each mutant lysozyme.

Cell adhesion activity was determined using baby hamster kidney (BHK) cells as described (6, 11). The amount of lysozyme adsorbed onto a plate was estimated by subtracting the unadsorbed amount from the added amount of lysozyme in the assay. The unadsorbed amount was determined based on the lytic activity remaining in the sample solution after binding to the plate. The results indicated that the adsorption efficiency was in the range of 60–80 % at the concentration shown in *Figure 2*, for native and mutant lysozymes.

Results and discussion

Previously a cell adhesive protein 74RGD4 was constructed, by inserting the RGDS sequence between ^{74}Val and ^{75}Asn in a long loop consisting of residues of ^{65}Cys to ^{81}Cys in human lysozyme (5). The backbone structure of the 74RGD4 lysozyme refined by X-ray crystallography is shown in *Figure 1*. To find an RGD introduction site in a different region than the long loop of the lysozyme molecule, three lysozyme variants were constructed by means of site-directed mutagenesis, namely 14RGD4 with RGDS in place of RLGM (residues 14 to 17) in an α-helix, 41RGD4 with RGDS in place of RATN (residues 41 to 44) in a β-sheet, and 47RGD4 with RGDS in place of AGDR (residues 47 to 50) in a β-turn. The 47RGD4 mutant was secreted with high efficiency in our yeast expression system (*Table 1*), while the 14RGD4 and 41RGD4

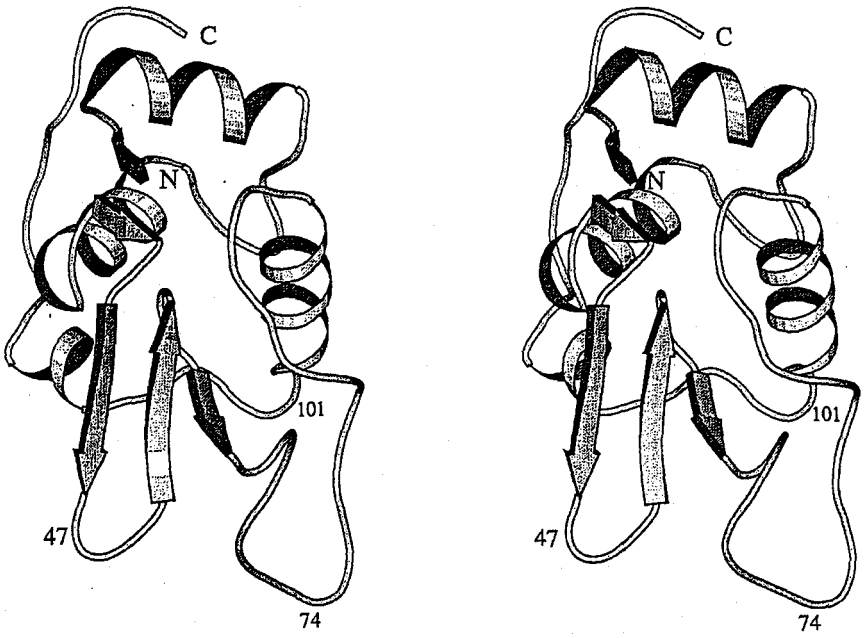

Figure 1. Stereo drawing of the backbone structure of the 74RGD4 lysozyme. The picture was produced with the program MOLSCRIPT (20) using the atomic coordinates of 74RGD4 (5). The α-helix and β-strand parts are shown as a ribbon model. The RGD introduction sites in this study are labeled.

Table 1. Production and relative lytic activity of each mutant lysozyme

Lysozyme	Productivity [a] (mg/l)	Relative lytic activity (%)
Native	5.3	100
74RGD4	6.3	109
47RGD4	4.5	92
(47,74)RGD4	6.7	83

[a]Based on lytic activity in the culture supernatant.

mutants failed to be fold correctly, and were not secreted from the yeast cells. The lytic activity of 47RGD4 as well as 74RGD4 was nearly the same as that of the native form (*Table 1*), indicating that these RGD introduction had no effect on the active cleft of human lysozyme. The successful folding of these fully active mutants is probably due to the distant location sites from the active cleft (12).

Using baby hamster kidney (BHK) cells, 47RGD4 was shown to possess the same level of adhesion activity as that of 74RGD4 (*Figure 2*). Another mutant, 101RGD4, was also produced by inserting RGDS for RDPQ (residues 101 to 104) in turn-like region of the lysozyme molecule. In the cell adhesion assay, however, the 101RGD4 mutant was inactive. This is probably because the RGD region of the 101RGD4 lysozyme fails to have a β-turn structure owing to the location in the bottom of a loop consisting of residues of ^{101}Arg to ^{110}Val (12) (*Figure 1*). On the other hand,

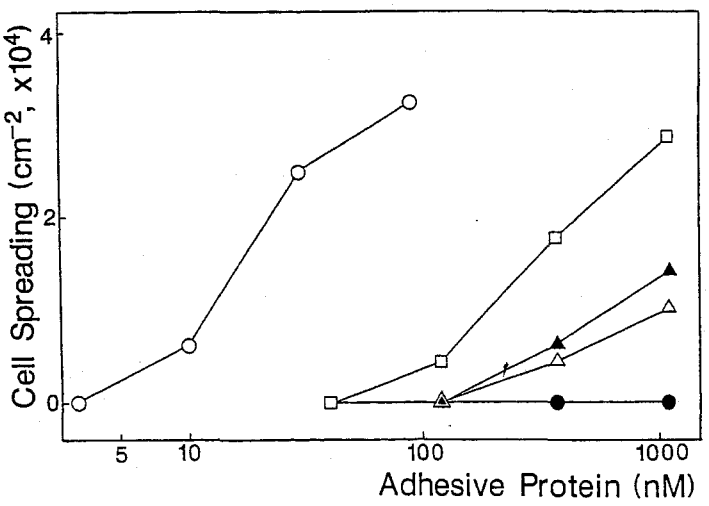

Figure 2. Cell adhesion assay on the substrates coated with each mutant lysozyme. The plastic substrates were coated with different concentrations of vitronectin (open circle), native lysozyme (closed circle), 74RGD4 (open triangle), 47RGD4 (closed triangle), and (47,74)RGD4 (open square). BHK cells were incubated on the substrates for 60 min at 37 °C in a CO_2 incubator. The cell adhesion activity was expressed as the number of cells adhering to unit surface area (cm^2).

the RGD sequence of the 47RGD4 mutant is destined to assume a stable turn conformation, since the two β-strands, ^{42}Ala–^{46}Asn and ^{51}Ser–^{55}Gly, connected by the RGDS (residues 47 to 50) to form a rigid β-sheet (*Figure 1*). Thus, these results suggest that the introduction of a functional RGD sequence is acceptable only in a certain β-turn region of human lysozyme.

This structural information about the RGD introduction site is in good accordance with the experimental studies on the functional conformation of the RGD region in several proteins. Recently the X-ray crystal structure of the CRGDSC-inserted lysozyme, named Cys-RGD4, was solved. The RGD sequence in this protein resides within a stable type II′ β-turn, with Gly and Asp in positions 2 and 3 of the turn (8). The fibronectin type III domain from human tenascin (13), and the leech protein decorsin (14) also have type II' β-turn structures in their RGD regions. In addition, a flexible conformation of RGD has been reported in the 74RGD4 lysozyme (5), the tenth type III module of human fibronectin (15), and the distintegrins, a family of integrin antagonists from snake venoms (16, 17). In these cases, the RGD region, which is highly flexible by nature, could assume a rigid turn conformation when it binds to integrins to form a ligand-receptor complex. It is also possible to consider that the RGD region has a type II' β-turn by itself, and that it was ill-defined because of its location at the apex of a flexible, long loop.

I finally constructed (47,74)RGD4, a mutant containing RGD at two sites, by combining the NH_2-terminal domain of 47RGD4 and the COOH-terminal domain of 74RGD4, as described in '*Materials and methods*'. The (47,74)RGD4 lysozyme was successfully secreted with full lytic activity (*Table 1*). As shown in *Figure 2*, the (47,74)RGD4 lysozyme exhibited even higher adhesion activity to BHK cells than that

of 74RGD4 or 47RGD4. It was also confirmed that this activity is nearly equal to 10 % of human vitronectin activity (*Figure 2*). The difference might be reasonable, if I consider that the natural cell adhesive proteins including vitronectin, possess a second binding site besides the RGD region to exhibit the optimum affinity for the integrins (17–19). The cell adhesion activities of the three mutants, 74RGD4, 47RGD4 and (47,74)RGD4, were completely inhibited by the addition of either GRGDSP peptide or polyclonal antibody against vitronectin receptor, as was the case for the vitronectin activity (data not shown). The results indicate that the cell adhesion signals in these mutant lysozymes are transduced to BHK cells through the interaction with the vitronectin receptor, the integrin $\alpha_v\beta_3$.

The high cell adhesion activity of the (47,74)RGD4 mutant suggests that both of the introduced RGD sequences are functional. This speculation was further supported by additional experiments, in which each substitution of Glu for Asp in the two RGD-containing regions of (47,74)RGD4 results in a significant decrease in the cell adhesion activity (data not shown). In addition, adhesion activity in a mixture of 74RGD4/47RGD4 (1:1) was similar to that of (47,74)RGD4, when expressed against their RGD concentrations (data not shown). These results suggest that the higher activity of (47,74)RGD4 is due to the increased concentration of the RGD sites, namely the additive effect of 74RGD4 and 47RGD4.

I have reported the successful construction of (47,74)RGD4, a cell adhesive lysozyme with two functional RGD sequences, and discussed the structural feature of the possible introduction site of RGD in human lysozyme. According to the model structure of the lysozyme molecules (*Figure 1*), the two RGD introduction sites are located at a considerable distance (19.4 Å). Thus the (47,74)RGD4 mutant may be

useful as a functional cross-linker in RGD dependent cell-to-cell interactions, differently from 74RGD4 or 47RGD4.

Acknowledgments

I thank Dr. M. Ikehara for his interest and encouragement throughout this work. I also thank Dr. M. Matsushima for helpful discussions.

References

1. Pierschbacher, M. D., and Ruoslahti, E. (1984) *Nature* **309**, 30–33.
2. Suzuki, S., Oldberg, A., Hayman, E. G., Pierschbacher, M. D., and Ruoslahti, E. (1985) *EMBO J.* **4**, 2519–2524.
3. Watt, K. W. K., Cottrall, B. A., Strong, D. D., and Doolittle, R. F. (1979) *Biochemistry* **18**, 5410–5416.
4. Hynes, R. O. (1987) *Cell* **48**, 549–554.
5. Yamada, T., Matsushima, M., Inaka, K., Ohkubo, T., Uyeda, A., Maeda, T., Titani, K., Sekiguchi, K., and Kikuchi, M. (1993) *J. Biol. Chem.* **268**, 10588–10592.
6. Yamada, T., Uyeda, A., Kidera, A., and Kikuchi, M. (1994) *Biochemistry* **33**, 11678–11683.
7. Pierschbacher, M. D., and Ruoslahti, E. (1987) *J. Biol. Chem.* **262**, 17294–17298.
8. Yamada, T., Song, H., Inaka, K., Shimada, Y., Kikuchi, M., and Matsushima, M. (1995) *J. Biol. Chem.* **270**, 5687–5690.
9. Taniyama, Y., Yamamoto, Y., Kuroki, R., and Kikuchi, M. (1990) *J. Biol.*

Chem. **265**, 7570–7575.

10. Yoshimura, K., Toibana, A., Kikuchi, K., Kobayashi, M., Hayakawa, T., Nakahama, K., Kikuchi, M., and Ikehara, M. (1987) *Biochem. Biophys. Res. Commun.* **145**, 712–718.

11. Maeda, T., Oyama, R., Ichihara-Tanaka, K., Kimizuka, F., Kato, I., Titani, K., and Sekiguchi, K. (1989) *J. Biol. Chem.* **264**, 15165–15168.

12. Inaka, K., Taniyama, Y., Kikuchi, M., Morikawa, K., and Matsushima, M. (1991) *J. Biol. Chem.* **266**, 12599–12603.

13. Leahy, D. J., Hendrickson, W. A., Aukhil, I., and Erickson, H. P. (1992) *Science* **258**, 987–991.

14. Krezel, A. M., Wagner, G., Seymour-Ulmer, J., and Lazarus, R. A. (1994) *Science* **264**, 1944–1947.

15. Main, A. L., Harvey, T. S., Baron, M., Boyd, J., and Campbell, I. D. (1992) *Cell* **71**, 671–678.

16. Adler, M., Lazarus, R. A., Dennis, M. S., and Wagner, G. (1991) *Science* **253**, 445–448.

17. Saudek, V., Atkinson, R. A., and Pelton, J. T. (1991) *Biochemistry* **30**, 7369–7372.

18. Obara, M., Kang, M. S., and Yamada, K. M. (1988) *Cell* **53**, 649–657.

19. Hearly, J., Murayama, O., Maeda, T., Yoshino, K., Sekiguchi, K., and Kikuchi, M. (1995) *Biochemistry* **34**, 3948–3955.

20. Kraulis, P. J. (1991) *J. Appl. Crystallogr.* **24**, 946–950.

SECTION II

Integrin-specific tissue-type plasminogen activator engineered by introducing of the Arg-Gly-Asp sequence

Introduction

Tissue-type plasminogen activator (tPA) is a glycosilated serine protease of 68 kDa, and consists of five domains, namely finger, EGF-like, kringle 1, kringle 2, and protease domains (see *Figure 1*) (1, 2). It is an essential component of the vascular thrombolytic system, and converts plasminogen into plasmin, which in turn degrades fibrin clots and causes the dissolution of thrombi (3). Human tPA has been produced by recombinant DNA technology, and used as a thrombolytic agent for coronary thrombosis. Clinical trials, however, indicated that rapid and effective thrombolysis requires comparatively high doses of tPA because of its short half-life *in vivo* (4). Thus serious side effects, systemic plasmin generation and bleeding, are often observed in tPA-treated patients (4).

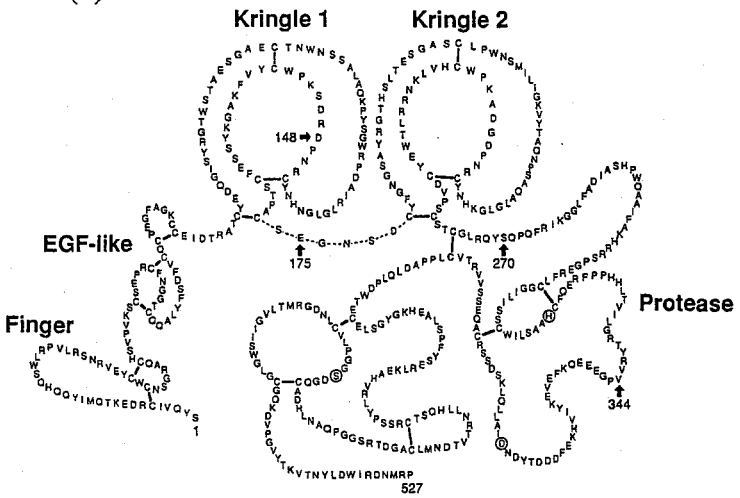

Figure 1. Illustration of the amino acid sequence of human tPA. The RGD introduction sites in this study are labeled and shown by the arrow. The circled residues indicate the catalytic triad in the protease domain of the tPA molecule. The solid bars indicate the potential disulfide bonds. This illustration is modified from that of Gething *et al.* (14).

The Arg-Gly-Asp (RGD) sequence is well-known as a site in cell adhesive proteins, such as fibronectin (5), vitronectin (6), and fibrinogen (7), for binding to their receptors, the integrins (8). In 1989, Maeda et al. inserted the RGD sequence into a truncated form of protein A, and succeeded in constructing an artificial cell adhesive protein A without destroying the intrinsic immunoglobulin-binding activity (9). With the same technology, human lysozyme was modified to possess an affinity for the integrins in addition to the intrinsic lytic activity (10, 11). In this study, introduction of a functional RGD sequence into the tPA molecule was investigated. Such tPA mutants are expected to bind specifically to platelet integrin, integrin $\alpha_{IIb}\beta_3$, which is one of the major components localized in thrombi, and thus cause the efficient dissolution of thrombi. Here I describe the construction of the integrin-specific tPA molecules, and their functional evaluation.

Materials and methods

Vector constructions

The pcD-tPA vector, with the human tPA gene inserted in the *Bam*HI site of pcDNAI/Amp (Invitrogen), was a generous gift from Drs. K. Igarashi and K. Kitano (Takeda Chemical Industries). Oligonucleotides were chemically synthesized using an automated DNA synthesizer (Model 380B, Applied Biosystems). The mutation was performed in M13tv18BtPA using the site-directed mutagenesis system Mutan-G (Takara Shuzo). The primer used for the construction of 148RGD-tPA, for example, was 5'-AACTACTGCAGAAACCCCCGCGGAGACTCAAAGC-3'. The underlined bases indicate mismatches. The sequence of the mutated gene was confirmed by dideoxy sequencing. The genes encoding the signal sequence and the mutated human

tPA were inserted in the *Bam*HI site of pcDNA/Amp to construct the expression vector.

Expression and purification of mutant human tPAs

The transient expression vector was introduced into COS-1 cells using the Lipofectamine reagent (Life Technologies, Inc.). Each of the tPA mutants was expressed according to the manufacturer's protocol except that the COS-1 cells were finally incubated in Dulbecco's modified Eagle's medium for 43 h at 37 °C. After the incubation with the serum-free medium, each culture supernatant was collected by centrifugation.

Secreted mutant tPAs were partially purified from the culture supernatants by chromatography on a column of lysine-Sepharose 4B (Pharmacia) (12). Each of the final preparation gave a protein band with of approximately 70 kDa on SDS-PAGE, which was shown to be derived from the tPA protein by the western blotting analysis.

Assay of tPA protein

The tPA protein was assayed by a sandwich method using a human tPA ELISA kit (Takara Shuzo), according to the manufacturer's protocol. Goat anti-human tPA immunoglobulin was used as the first antibody, and horseradish peroxidase (HRP)-conjugated goat anti-human tPA IgG was second antibody.

Direct chromogenic assay of tPA activity

The enzymatic activity of tPA was determined using the chromogenic substrate Spectrozyme tPA (American Diagnostica Inc.), which is cleaved directly by tPA at the arginine-*p*-nitroaniline bond (13). The assay was performed at 37 °C in 96-well EIA

plates, and the reaction progress was monitored by measuring the production of free *p*-nitroaniline spectrophotometrically at 405 nm (ε=9920 $M^{-1}cm^{-1}$) at 2 h intervals over a 10 h period. The standard reaction mixture contained 0.2 to 2.0 ng of tPA in a final volume of 0.2 ml. One enzyme unit (1 IU) is defined as the amount of tPA that causes the release of 1 μmol of *p*-nitroaniline per minute.

Indirect chromogenic assay of tPA activity

The indirect chromogenic assay was performed using the substrates Lys-plasminogen (American Diagnostica Inc.) and Spectrozyme PL (American Diagnostica Inc.) as described by Gething et al. (14). The standard reaction mixture contained 0.1 to 0.2 ng of tPA in a final volume of 0.1 ml. Under the conditions used, the addition of soluble fibrin (25 μg/ml DESAFIB, American Diagnostica Inc.) stimulated the tPA activity about 20-fold, regardless of native and mutant tPAs.

Binding assay of mutant tPAs to integrin $\alpha_{IIb}\beta_3$

Integrin $\alpha_{IIb}\beta_3$ was purified from outdated human platelets, as described previously (15). The platelet integrin $\alpha_{IIb}\beta_3$ (0.1 mg/ml) was diluted 1:100 with Triton X-100-free solution containing 20 mM Tris-HCl, 150 mM NaCl, 1 mM $CaCl_2$, 0.02 % NaN_3, and 1 mg/ml BSA, pH 7.4 added to 96-well EIA plates at 0.1 ml (0.1 μg) per well, and incubated overnight at 4 °C. The wells were incubated with 0.15 ml of blocking solution (50 mM Tris-HCl, 100 mM NaCl, 2 mM $CaCl_2$, 0.02 % NaN_3, and 35 mg/ml BSA, pH 7.4) for 2 h at 30 °C, followed by two washes with buffer A (50 mM Tris-HCl, 100 mM NaCl, 2 mM $CaCl_2$, 0.02 % NaN_3, and 1 mg/ml BSA, pH 7.4). The mutant tPAs or the native tPA were added at different concentrations in 0.1 ml of buffer A per

well, and incubated for 3 h at 30 °C. After two washes with buffer A, the bound tPA was quantitated with HRP-conjugated goat anti-human tPA IgG, using tPA bound by immobilized goat anti-human tPA immunoglobulin as a standard (see '*assay of tPA protein*'). Non-specific binding of the tPAs to the integrin was measured by determining the binding of tPAs in the presence of 10 mM EDTA, because it chelates divalent cations that are required for the RGD-dependent binding to the integrin (16). The similar results on the non-specific binding were also obtained using 1 mg/ml GRGDSP (Peptide Institute, Inc.) as a competitor.

Enzymatic assay of mutant tPAs bound by integrin $\alpha_{IIb}\beta_3$

The binding reaction of the mutant tPAs to integrin $\alpha_{IIb}\beta_3$ immobilized on wells was performed, as described in '*Binding assay of mutant tPAs to integrin $\alpha_{IIb}\beta_3$*'. The enzymatic activity of the mutant tPAs bound by the integrin was determined, as described in '*Direct chromogenic assay of tPA activity*'.

Results and discussion

Four kinds of tPA mutants were constructed by introducing the Arg-Gly-Asp (RGD) sequence by means of site-directed mutagenesis. They are 148RGD-tPA with RGDS in place of DRDS (residues 148 to 151), 175RGD-tPA with RGDS in place of EGNS (residues 175 to 178), 270RGD-tPA with RGDS in place of SQPQ (residues 270 to 273), and 344RGD-tPA with RGDS in place of VPGE (residues 344 to 347) (*Figure 1*). These introduction sites were selected based on the following reason. First, they are located in the loop region of tPA (148RGD- and 344RGD-tPAs) or in the linker region between two domains of tPA (175RGD- and 270RGD-tPAs). Thus they should be

exposed on the surface of the tPA molecule, to allow access to the integrin receptors. Second, they are expected to have little effect on the tPA activity, which would enable us to construct an integrin-specific molecule with full tPA activity.

These four mutants as well as native tPA were expressed in COS-1 cells, and partially purified by lysine-Sepharose chromatography. The tPA proteins were quantified by a sandwich method using a tPA ELISA kit (Takara Shuzo). The amounts of the tPAs thus determined were in good agreement with the densitometric assay of the tPA band of approximately 70 kDa in the SDS-PAGE analysis of the partially purified preparations (data not shown). The results suggest that the native tPA and the four tPA mutants possess the same level of binding affinity for the goat anti-human tPA immunoglobulin in the ELISA kit. Therefore, the productivity of these tPAs by the COS-1 expression system was estimated by measuring the tPA protein in the culture supernatant with the tPA ELISA kit. As shown in *Table 1*, mutant tPAs and native tPA were successfully secreted with the same level of efficiency (ca. 2 μg/ml). *Table 1* also shows the amidolytic activity of these mutant tPAs, using the chromogenic Spectrozyme tPA as a substrate. The 148RGD-, 175RGD-, and 340RGD-tPAs were shown to possess tPA activity (18,000–22,000 IU/mg) nearly equal to that of the native

Table 1. Production and amidolytic activity of each mutant tPA

tPA	Productivity[a] (μg/ml)	Amidolytic activity[b] (IU/mg)
Native	1.75	19,000
148RGD-tPA	1.79	18,000
175RGD-tPA	1.74	22,000
270RGD-tPA	1.91	5,700
344RGD-tPA	2.30	20,000

[a]Estimated by measuring tPA protein in the culture supernatant with the tPA ELISA kit.
[b]Based on amidolytic activity and tPA amount in the partially purified preparation.

form (19000 IU/mg). In the indirect chromogenic assay (see *'Materials and methods'*), in addition, the three mutants and native form exhibited the same level of tPA activity (data not shown). These RGD introduction sites are distant from a catalytic triad of amino acids (^{322}His, ^{371}Asp, and ^{478}Ser) in the tPA molecule (17), and this would allow the successful folding of these mutants with full tPA activity. The low activity of 270RGD-tPA could be due to the location of the introduction site near ^{276}Ile, a residue that was previously shown by site-directed mutagenesis to have an effect on tPA activity (17). Thus, the RGDS introduction in the 270RGD-tPA molecule could change the conformation of the catalytic triad, resulting in the significantly decreased activity of 270RGD-tPA.

The binding affinity of these tPA mutants for platelet integrin $\alpha_{IIb}\beta_3$ was purified from outdated human platelets by chromatography on columns of ConA-Sepharose, GRGDSPK-Sepharose, and Sephacryl S-300, as described previously (15). After these steps, highly purified integrin $\alpha_{IIb}\beta_3$ was obtained with a yield of 0.5 mg/5 U of human platelets. I developed a binding assay system using the platelet integrin, as described in *'Materials and methods'*. The tPA bound by the integrin was quantitated with HRP-conjugated goat anti-human tPA IgG, using tPA bound by immobilized goat anti-human tPA immunoglobulin as a standard. To check the binding efficiency of tPA for the immunoglobulin, the amount of unbound tPA was determined based on the tPA activity remaining in the standard solution after binding to the immunoglobulin. The results indicated that the efficiency was more than 90 % at the concentrations (0.2 to 5 ng/0.1 ml, 2.8 to 70 fmol/well) used here, for both the native and mutant tPAs. The binding assay showed that the native tPA as well as the RGD-containing mutants can bind to the integrin $\alpha_{IIb}\beta_3$ (*Figures 2A–2C*). However, the addition of 10 mM EDTA (or

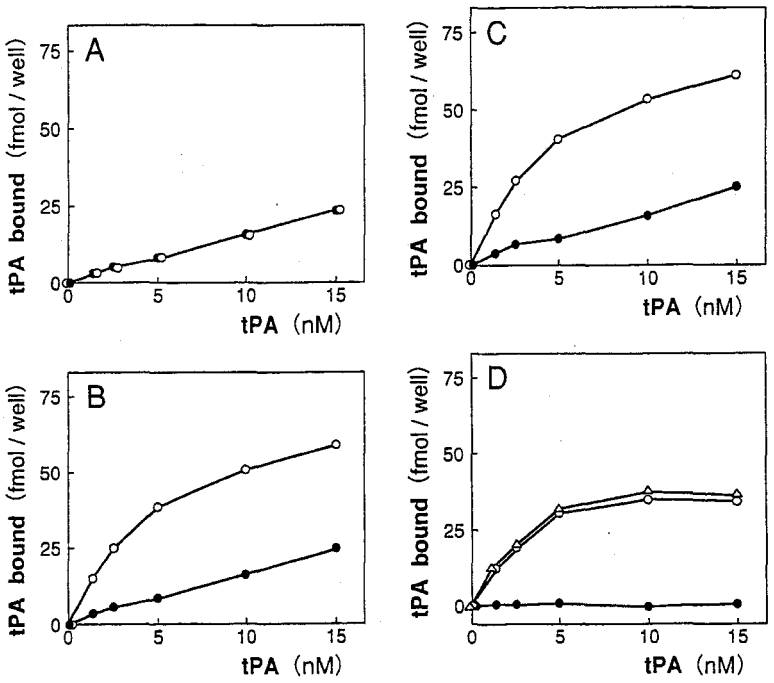

Figure 2. Binding assay of mutant tPAs to integrin $\alpha_{IIb}\beta_3$. The binding reaction of native tPA (A), 148RGD-tPA (B), and 270RGD-tPA (C) to integrin $\alpha_{IIb}\beta_3$ was performed in the presence of 2mM $CaCl_2$ (open circle) or 10 mM EDTA (closed circle), as described under *'Materials and methods'*. The tPA bound by the integrin was quantified with HRP-conjugated goat anti-human tPA IgG, as described in the text. (D) Evaluation of the RGD-dependent binding of native tPA (closed circle),. 148RGD-tPA (open circle), 270RGD-tPA (open triangle) to integrin $\alpha_{IIb}\beta_3$. The binding specific for the RGD sequence was calculated by subtracting the non-specific binding in the presence of 10 mM EDTA.

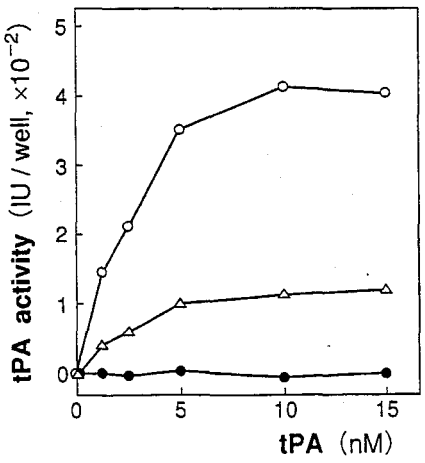

Figure 3. Enzymatic assay of mutant tPAs bound by integrin $\alpha_{IIb}\beta_3$. The binding reaction of native tPA (closed circle), 148RGD-tPA (open circle), and 270RGD-tPA (open triangle) to integrin $\alpha_{IIb}\beta_3$ was performed, as in the case of *Figure 2*. The tPA activity of the mutants bound RGD-dependently by the integrin was calculated by subtracting the tPA activity due to non-specific binding in the presence of 10 mM EDTA.

1 mg/ml GRGDSP) to the assay system had no effect on the binding of the native tPA (*Figure 2A*), indicating that the binding is non-specific. Thus the binding specific for the RGD sequence of the mutants was evaluated by subtracting the non-specific binding in the presence of 10 mM EDTA (or 1 mg/ml GRGDSP). *Figure 2D* clearly shows that the 148RGD- and 270RGD-tPAs can interact with the integrin in an RGD-dependent manner, and that the two mutants possess the same level of binding affinity, exhibiting a K_d of approximately 2 nM. It is noteworthy that the nanomolar affinity of these mutants for the integrin $\alpha_{IIb}\beta_3$ is 100-fold higher than that of an RGD-containing peptide such as GRGDS (18). Two other mutants , the 175RGD- and 344RGD-tPAs, exhibited only the non-specific binding to the integrin, as was the case of the native tPA (data not shown).

Recently the X-ray crystal structure of the GRGDSC-inserted lysozyme, named Cys-RGD4, was solved. The RGD sequence in this protein resides within a stable type II′ β-turn, with Gly and Asp in positions 2 and 3 of the turn (11). The fibronectin type III domain from human tenascin (19), and the leech protein decorsin (20) also have type II′ β-turn structures in their RGD regions. These results and my present observations suggest that the RGD regions of the two mutants, the 148RGD- and 270RGD-tPAs, assume a turn conformation, resulting in the high affinity for the integrin. Based on the structural analysis of the kringle 2 domain of tPA (21), the RGD introduction site in the 148RGD-tPA mutant is considered to lie not on a turn, but on a conformationally flexible loop. Therefore, the RGD region of the mutant, which is highly flexible by nature, could assume a stable turn when it binds to the integrin to form a ligand-receptor complex. Such a flexible conformation of RGD has been reported in the 74RGD4 lysozyme (10), the tenth type III module of human fibronectin (22), and the disintegrins, a family of the integrin antagonists from snake venoms (23, 24).

The two tPA mutants possess a high level of binding affinity for the integrin $\alpha_{IIb}\beta_3$, in addition to the tPA enzymatic activity. Next it was examined whether they exhibit the tPA activity when they interact with the integrin immobilized on wells. The tPA activity of the mutants bound RGD-dependently by the integrin was calculated by subtracting the tPA activity due to the non-specific binding in the presence of 10 mM EDTA (or 1 mg/ml GRGDSP). As shown in *Figure 3*, the bound 148RGD-tPA clearly exhibits enzymatic activity, while the activity of the bound 270RGD-tPA is 3- to 4-fold lower. The 148RGD-tPA bound by the integrin retained full activity (17,000–20,000 IU/mg), as estimated by the amount (*Figure 2D*) and the activity (*Figure 3*) of tPA per well. The low activity of the 270RGD-tPA bound by the integrin is in good accordance with that of the free form (*Table 1*).

In the present investigation, I have shown that the 148RGD-tPA, an RGD-introduced tPA mutant, possesses high affinity for the integrin $\alpha_{IIb}\beta_3$ as well as full tPA activity. An effort to target urokinase-type plasminogen activator to blood thrombi, by conjugating the enzyme to the Fab′ fragment of a monoclonal antibody against the platelet integrin, has been reported (25). The covalent coupling yields a molecule that is 25-fold more potent in a plasma clot lysis assay than the native urokinase. The bi-functional 148RGD-tPA molecule described here, due to its novel binding property, might also exhibit enhanced affinity for platelet-rich thrombi, and thus would be useful as an improved thrombolytic agent for coronary thrombosis.

Acknowledgments

I thank Drs. K. Igarashi and K. Kitano for the gift of the human tPA gene. I also thank Dr. M. Ikehara for his support, and Drs. M. Matsushima and K. Nishikawa for

helpful discussions throughout this work.

References

1. Pennica, D., Holmes, W. E., Kohr, W. J., Harkins, R. N., Vehar, G. A., Benett, W. F., Yelverton, E., Seeburg, P. H., Heyneker, H. L., Goeddel, D. V., and Collen, D. (1983) *Nature* **301**, 214–221.

2. Harris, T. J. R., Patel, T., Marston, F. A. O., Little, S., Emtage, S., Opdenakker, G., Volckaert, G., Rombauts, W., Billiau, A., and de Somer, P. (1986) *Mol. Biol. Med.* **3**, 279–292.

3. Collen, D. (1980) *Thromb. Haemostasis* **43**, 77–89.

4. Boville, E. G., Terrin, M. L., Stump, D. C., Berke, A. D., Frederick, M., Collen, D., Feit, F., Gore, J. M., Hillis, L. D., Lambrew, C. T., Leiboff, R., Mann, K. G., Markis, J. E., Pratt, C. M., Sharkey, S. W., Sopko, G., Tracy, R. P., and Chesebro, J. H. (1991) *Annu. Int. Med.* **115**, 256–265.

5. Pierschbacher, M. D., and Ruoslahti, E. (1984) *Nature* **309**, 30–33.

6. Suzuki, S., Oldberg, A., Hayman, E. G., Pierschbacher, M. D., and Ruòslahti, E. (1985) *EMBO J.* **4**, 2519-2524.

7. Watt, K. W. K., Cottrall, B. A., Strong, D. D., and Doolittle, R. F. (1979) *Biochemistry* **18**, 5410–5416.

8. Hynes, R. O. (1987) *Cell* **48**, 549–554.

9. Maeda, T., Oyama, R., Ichihara-Tanaka, K., Kimizuka, F., Kato, I., Titani, K., and Sekiguchi, K. (1989) *J. Biol. Chem.* **264**, 15165–15168.

10. Yamada, T., Matsushima, M., Inaka, K., Ohkubo, T., Uyeda, A., Maeda, T., Titani, K., Sekiguchi, K., and Kikuchi, M. (1993) *J. Biol. Chem.* **268**,

10588–10592.

11. Yamada, T., Song, H., Inaka, K., Shimada, Y., Kikuchi, M., and Matsushima, M. (1995) *J. Biol. Chem.* **270**, 5687–5690.

12. Radcliffe, R., and Heinze, T. (1978) *Arch. Biochem. Biophys.* **189**, 185–194.

13. Magnotti, R. A., Jr. (1988) *Anal. Biochem.* **170**, 228–237.

14. Gething, M. J., Adler, B., Boose, J. A., Gerard, R. D., Madison, E. L., McGookey, D., Meidell, R. S., Roman, L. M., and Sambrook, J. (1988) *EMBO J.* 7, 2731–2740.

15. Yamada, T., Uyeda, A., Kidera, A., and Kikuchi, M. (1994) *Biochemistry* **33**, 11678–11683.

16. Pytela, R., Pierschbacher, M. D., Argraves, S., Suzuki, S., and Ruoslahti, E. (1987) *Methods Enzymol.* **144**, 475–489.

17. Paoni, N. F., Chow, A. M., Pena, L. C., Keyt, B. A., Zoller, M. J., and Bennett, W. F. (1993) *Protein engng.* **6**, 529–534.

18. Dennis, M. S., Henzel, W. J., Pitti, R. M., Lipari, M. T., Napier, M. A., Deisher, T. A., Bunting, S., and Lazarus, R. A. (1989) *Proc. Natl. Acad. Sci. USA* **87**, 2471–2475.

19. Leahy, D. J., Hendrickson, W. A., Aukhil, I., and Erickson, H. P. (1992) *Science* **258**, 987–991.

20. Krezel, A. M., Wagner, G., Seymour-Ulmer, J., and Lazarus, R. A. (1994) *Science* **264**, 1944–1947.

21. de Vos, A. M., Ultsch, M. H., Kelley, R. F., Padmanabhan, K., Tulinsky, A., Westbrook, M. L., and Kossiakoff, A. A. (1992) *Biochemistry* **31**, 270–279.

22. Main, A. L., Harvey, T. S., Baron, M., Boyd, J., and Campbell, I. D. (1992)

Cell **71**, 671–678.

23. Adler, M., Lazarus, R. A., Dennis, M. S., and Wagner, G. (1991) *Science* **253**, 445–448.

24. Saudek, V., Atkinson, R. A., and Pelton, J. T. (1991) *Biochemistry* **30**, 7369–7372.

25. Bode, C., Meinhardt, G., Runge, M. S., Freitag, M., Nordt, T., Arens, M., Newell, J. B., Kübler, W., and Haber, E. (1991) *Circulation* **84**, 805–813.

CHAPTER II

Proteolytic analysis of domain organization of soluble extracellular region of metabotropic glutamate receptor subtype 1

Introduction

In contrast to the classical G-protein coupled receptors (GPCRs), metabotropic glutamate receptors (mGluRs) contain large extracellular regions (~600 amino acids) (1, 2). The NH_2-terminal extracellular regions have amino acid sequence similarity to that of leucine-, isoleucine-, valine-binding protein (LIVBP), one of the bacterial periplasmic binding proteins (3). The LIVBP-like region is followed by a cysteine-rich region that precedes the first transmembrane segment. LIVBP-like regions are also found in the $GABA_B$ receptor (4), the putative pheromone receptor (5, 6) and the calcium sensing receptor (7). The cysteine-rich region is not shared by the bacterial binding proteins and the $GABA_B$ receptor.

Previously the whole extracellular region of mGluR1 was produced in a soluble form (8). The receptor protein secreted into the culture medium retained the ligand binding affinity and selectivity comparable with those of the full-length membrane bound receptor. Interestingly the soluble receptor of mGluR1 was a cysteine-linked dimer. Dimer or oligomer forms of other subtypes of mGluRs, mGluR5 (9) and mGluR4 (10), or of calcium sensing receptor (11, 12) have been also reported. However, the precise mechanism of ligand binding to the mGluR is unknown. It is still unclear whether glutamate binds to mGluRs in an analogous way to the Venus' flytrap model proposed in the bacterial binding proteins (13), whereby the ligand bound to one lobe is trapped to another lobe by the bending motion of the hinge region. Role(s) of

dimerization of mGluR1 in ligand binding and signal transmission remain to be elucidated.

In this study, as the first step for delineating ligand binding core of mGluR1, the domain organization of the extracellular region was defined. I have performed proteolysis experiments of the purified extracellular region of mGluR1. The new construct, designed according to the protease sensitive boundary, produced the shorter soluble receptor lacking the cysteine-rich region. It was determined a ligand-binding constant and a maximal binding value of the soluble receptor that consists solely of the LIVBP-like domain in comparison with that of the soluble receptor encompassing the whole extracellular domain. I also examined protease sensitivity of the soluble receptors with and without ligand.

Materials and methods

Materials

Linear gradient polyacrylamide gels were MULTIGEL obtained from Daiichi Pure Chemicals (Tokyo, Japan). Ethylene glycol bis(succinimidylsuccinate) (EGS) was obtained from Pierce (Rockford, IL). *N*-Cyclohexyl-3-aminopropanesulfonic acid (CAPS) and phenylmethylsulfonyl fluoride (PMSF) were purchased from WAKO Pure Chemical Industries (Osaka, Japan). Type XI trypsin, diphenyl carbamyl chloride treated from bovine pancreas, was obtained from Sigma Aldrich Fine Chemicals (St. Louis, MO). All other reagents were of analytical grade.

Construction of transfer vectors for expression of mGluRs in insect cells

Both transfer vectors, pVLmGluR113 and pVLmGluR114, were constructed

from pmGluR108 (8). pVLmGluR113 was made as follows. A set of complementary oligonucleotides, HJ110 (5'-CACAGGCTGTGAGCCCATTCCTGTCCGTTATCTTGAGTGGAGTGACATAGAATAGTGAT-3') and HJ111 (5'-CTAGATCACTATTCTATGTCACTCCACTCAAGATAACGGACAGGAATGGGCTCACAGCCTGTGAGCT-3'), were annealed and cloned into the *Sac*I/*Xba*I-digested fragment of pmGluR108. pVLmGluR114 was made as follows. Polymerase chain reaction (PCR) was done with primers TO1 (5'-CATCAATGCCATCTATGCCATGGC-3') and HJ112 (5'-TCTAGATTACTAAGATCGTACCATTCCGCTTTTGTTC-3') using pmGluR108 as a template. TO1 contains an *Nco*I site. HJ112 contains an *Xba*I site. The PCR product was digested with *Nco*I and *Xba*I and was cloned into the *Nco*I/*Xba*I-digested fragment of pmGluR108. All of the above PCR products were entirely sequenced.

Cell culture

Recombinant baculoviruses were prepared using transfer vectors described above. Baculovirus infection was performed as described previously (8). Briefly, after being infected with baculoviruses for mGluR113 and mGluR114, insect cells (*Trichoplusia ni* BTI-TN-5B1-4 (High Five)) were incubated in Express Five™ (GIBCO BRL, Life Technologies, Inc., Rockville, MD) serum-free medium supplemented with 18 mM glutamine for four or five days.

Purification of soluble mGluRs

mGluR113 and mGluR114 were purified from culture medium of the insect

cells infected with baculovirus for each protein. Concentration of the culture medium and immunoaffinity column step were performed as described previously (8), except that 100 mM CAPS buffer (pH 11) containing 200 mM NaCl was used at the elution from the immunoaffinity column. After being neutralized with 2 M 2-[4-(2-hydroxyethyl)-1-piperazinyl]ethanesulfonic acid (Hepes), pH 7.5, and five-times diluted with 10 mM Hepes, pH 7.5, the sample was applied on Resource Q (Amersham Pharmacia Biotech) fitted to ÄKTA Explorer 10S (Amersham Pharmacia Biotech) equilibrated with 10 mM Hepes, pH 7.5, and eluted by NaCl at a gradient from 0 to 1.2 M. The yield of purification of mGluR113 and mGluR114 were around 0.1 mg/100 ml of culture medium.

Immunoblotting

Essentially the same as described previously (8). Culture medium was separated by SDS-polyacrylamide gel electrophoresis (PAGE) and electroblotted onto a nitrocellulose membrane (Schleicher & Schuell). mGluRs were identified by using the monoclonal antibody (MAb) mG1Na-1 (8, 14, 15) and anti-(mouse IgG)-conjugated alkaline phosphatase (Promega). Color development was done by a commercial detection kit (Promega).

Cross-linking procedure

The cross-linker, EGS, was dissolved at 20 mM in dimethylsulfoxide and diluted into the protein solution to give the final concentration of 1 mM. The reaction proceeding at 25 °C for 30 min was stopped by the addition of Tris-HCl buffer from a 1 M stock solution at pH 7.5 and a further incubation was conducted at 25 °C for 15 min.

The cross-linked material was analyzed by 4–20 % SDS-PAGE and silver-stained (WAKO Pure Chemical Industries).

Ligand binding

Ligand binding was performed with the polyethylene glycol (PEG) precipitation method as described previously (16). Briefly, 20 nM of [^{3}H]quisqualate (323 GBq/mmol) (a gift from BANYU Tsukuba Research Institute) and purified mGluR113 and mGluR114 were mixed in 150 μl of a binding buffer (40 mM Hepes, pH 7.5 containing 2.5 mM $CaCl_2$) at 4 °C for 1 h. After the binding reaction, 6 kDa PEG was added to the sample at the concentration of 15 % with 3 mg/ml of γ globulin. Precipitated material was washed twice with 1 ml of 8 % 6kDa PEG and dissolved in 1 ml of water. After addition of 14 ml Scintisol EX-H (WAKO Pure Chemical Industries), the radioactivity was counted in the scintillation counter. Binding data was analyzed by the software of Prism II (Graphpad Software, San Diego, CA). Saturation binding curves were fitted to a one-site binding model and K_d and B_{max} values were calculated.

Trypsin digestion and protein sequencing

Purified protein was digested in 10 mM Hepes, pH 7.5, with different concentrations of trypsin. Reaction was stopped with 0.01 mM PMSF and sample buffer. Aliquot was not heated and was subjected to SDS-PAGE. The gel was electroblotted onto a polyvinylidene difluoride membrane (Trans-Blot Transfer Medium, Bio-rad), stained with Coomassie Brilliant Blue R250 (PAGE Blue83, Daiichi Pure Chemicals), and destained with 20 % methanol. The protein bands were excised and subjected to automated Edman degradation by an Applied Biosystems Procise model 492 protein

sequencer (Applied Biosystems).

Native PAGE

Trypsin-digested samples were analyzed by a 4–20 % linear gradient polyacrylamide gel not containing SDS in the gel matrix. SDS was not included in either the running buffer or the sample buffer. Gels were Coomassie stained. Molecular weight standards were from Daiichi Pure Chemicals.

Low angle rotary shadowing

The purified mGluRs in 50 mM Hepes, pH 7.5, was equilibrated with glycerol (up to 50 % (v/v)). Final concentration of the protein was 50 μg/ml each. 50 μl of the sample was sprayed onto mica surface cleaved freshly by using a painter's airbrush (Olympus Model SP-B, f 0.18 mm). Then, the sample on the mica was rapidly brought into a freeze-etching device equipped with a large turbo pump (FR 7000, Hitachi, Mito, Japan), dried for 10 min (room temperature) in vacuum ($1x10^{-6}$ Pa) and then cooled down to –100 °C. Subsequently, specimens were rotary shadowed with platinum by an electron gun positioned at an angle of 2.5 ° to the mica surface and followed by carbon evaporation. Shadowed films were removed from the mica by slowly soaking the mica into water, mounted on copper grids and examined under a JEOL 100CX electron microscope (JEOL Co., Ltd., Tokyo).

Results

Figure 1 shows a schematic view of the transfer vectors, pVLmGluR113 and pVLmGluR114, used for making the recombinant viruses for mGluR113 and mGluR114. pVLmGluR113 encodes complementary DNA (cDNA) corresponding to the region ^{1}Met–^{592}Glu of the primary amino acid sequence of mGluR1. pVLmGluR114 encodes cDNA corresponding to the region ^{1}Met–^{522}Ser.

mGluR108 that was used in our previous study (8) encoded the amino acid region identical with that of pVLmGluR113 and six histidine codons at its COOH-

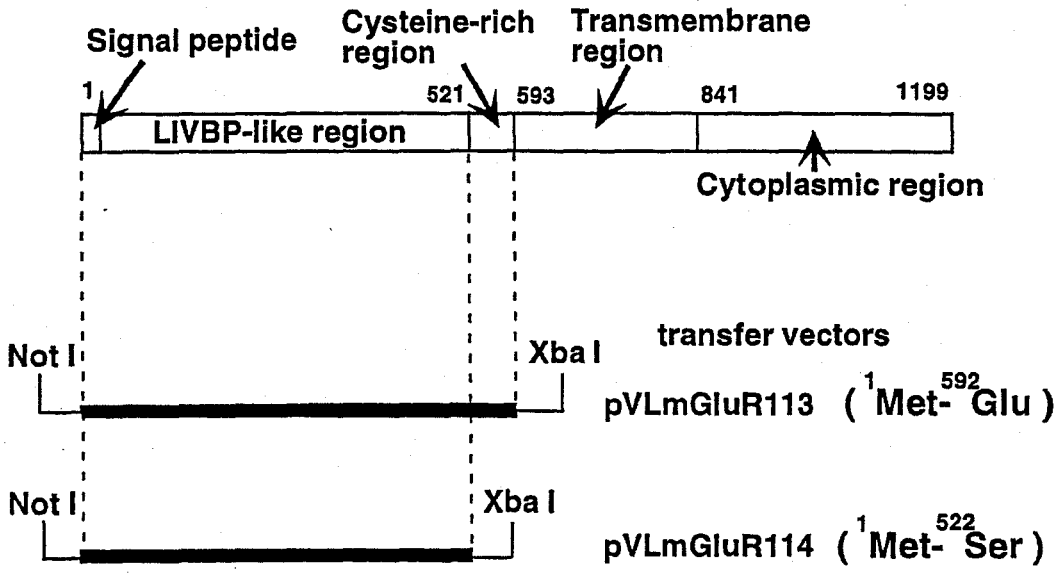

Figure 1. Schematic diagram of the expression construct of the transfer vectors in insect cells. Full-length wild type mGluR1 was presented as a diagram according to its primary amino acid sequence deduced from mGluR1cDNA (1). The numerical positions of amino acid residues of mGluR1 are indicated. Functional regions are boxed. Inserts of transfer vectors, pVLmGluR113 and pVLmGluR114, used in this study are presented according to the primary sequence of mGluR1. pVLmGluR113 encodes cDNA corresponding to the entire extracellular region consisting of a signal sequence, an LIVBP-like region and a cysteine-rich region. pVLmGluR114 is devoid of the sequence corresponding to COOH-terminal 70 amino acids out of pVLmGluR113. *Not*I-*Xba*I fragments were ligated into pVL1392.

terminus. In this study, a histidine tag-sequence of pmGluR108 was omitted in pVLmGluR113. In order to understand the domain organization of the mGluR1 extracellular region, I purified the soluble receptor protein, mGluR113, from culture medium by an immunoaffinity column as described previously (8). I first determined the NH_2-terminal amino acid sequence of soluble receptor protein, mGluR113, that was generated by removal of a signal peptide and found that mGluR113 began with a residue ^{33}Ser. Proteinase digestion was then performed using the purified mGluR113 (*Figures 2A* and *2B*). Limited proteolysis of mGluR113 by trypsin gave rise to at least five major bands. Each of these bands (designated as *fragments 1–5*) were excised from a polyvinylidene difluoride blot and sequenced at the NH_2-terminal end by Edman degradation. The NH_2-terminal amino acid sequence of the 15 kDa band (*fragment 4*) was identical with that of mGluR113. NH_2-terminal sequencing of the 50 kDa band (*fragment 2*) revealed that the digestion site was ^{139}Arg before ^{140}(C)LPDG. Thus the 15 kDa band (*fragment 4*) was residues 33 to 139 and the 50 kDa band (*fragment 2*) was residues 140 to 592. The NH_2-terminal sequence of an 8 kDa band (*fragment 5*), which was faintly observed by limited digestion without dithiothreitol (DTT) but was clearly visible in the lanes of samples digested in the presence of 1 mM DTT, disclosed the other trypsin sensitive site, ^{521}Arg before ^{522}SV(C)SE. Thus the 8 kDa band (*fragment 5*) was residues 522 to 592. A 42 kDa band (*fragment 3*) corresponded to residues 140 to 521. A 57 kDa band (*fragment 1*) was the intermediate that resulted from initial digestion at ^{521}Arg. The site ^{521}Arg seemed to be more accessible in the presence of DTT. Although mass spectroscopic analysis or amino acid content calculation is needed for strict identification of each band, I summarized my interpretation of the results (*Figure 2B*) and proceeded to the next experiments.

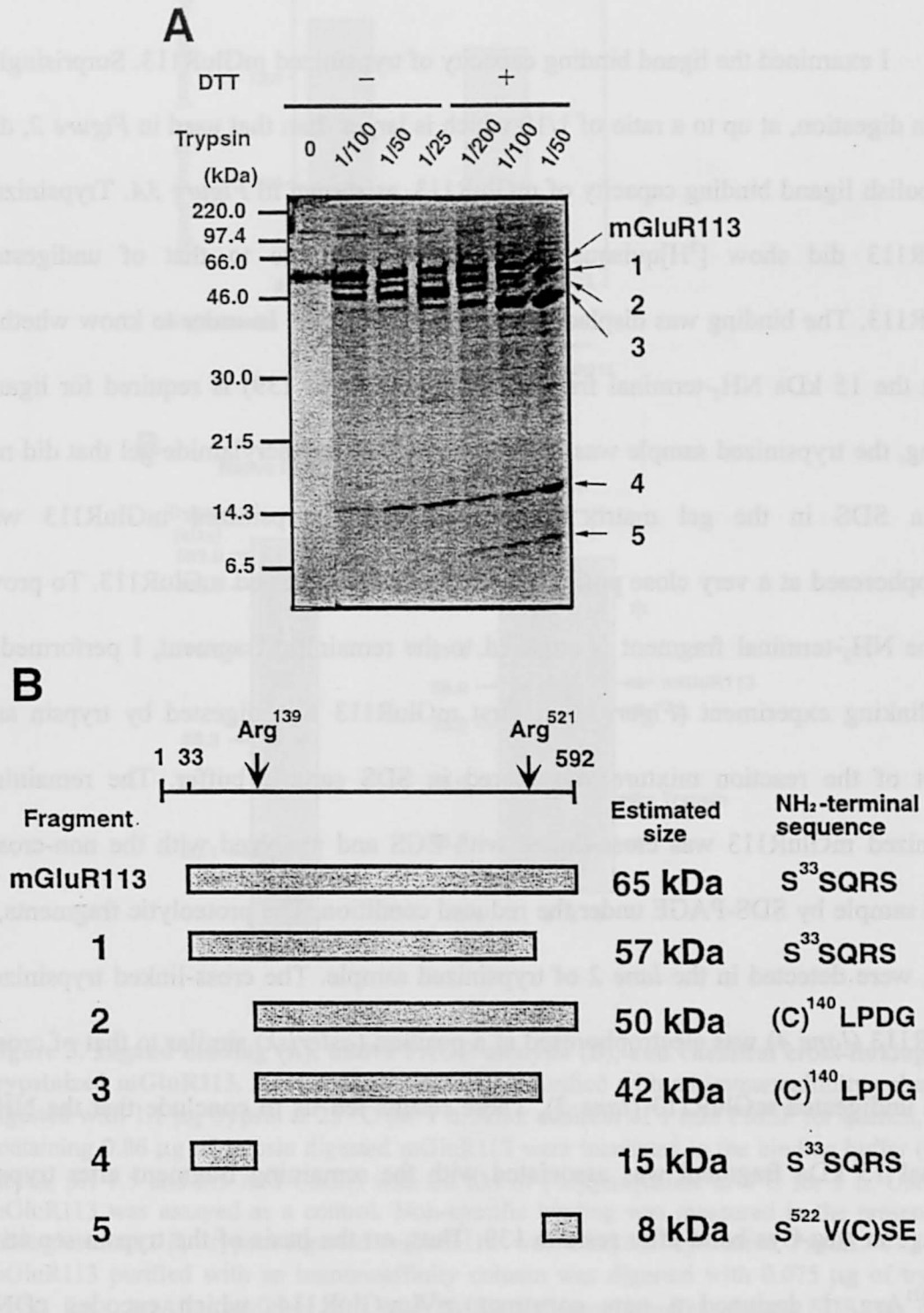

Figure 2. Trypsin digestion (A) and proteolytic cleavage mapping (B) of the soluble mGluR113. *A*, 13.6 µg of immunoaffinity-purified mGluR113 was digested with the indicated ratio (w/w) of trypsin at 25 °C for 1 h, loaded on a 15–25 % gradient gel and Coomassie stained. Proteolytic fragments were labeled *1–5*. NH_2-terminal sequences of mGluR113 and the five tryptic fragments were determined as described in '*Materials and methods*'. *B*, the five fragments, *1–5*, are located relative to the primary amino acid sequence of mGluR1. NH_2-terminal sequences of mGluR113 and the fragments are shown. The vertical arrows indicate the trypsin cleavage sites.

I examined the ligand binding capacity of trypsinized mGluR113. Surprisingly, trypsin digestion, at up to a ratio of 1/10 which is larger than that used in *Figure 2*, did not abolish ligand binding capacity of mGluR113, as shown in *Figure 3A*. Trypsinized mGluR113 did show [^{3}H]quisqualate binding comparable to that of undigested mGluR113. The binding was displaced by excess glutamate. In order to know whether or not the 15 kDa NH_2-terminal fragment (residues 33 to 139) is required for ligand binding, the trypsinized sample was loaded on a native polyacrylamide gel that did not contain SDS in the gel matrix (*Figure 3B*). The trypsinized mGluR113 was electrophoresed at a very close position to that of the undigested mGluR113. To prove that the NH_2-terminal fragment is attached to the remaining fragment, I performed a cross-linking experiment (*Figure 3C*). First mGluR113 was digested by trypsin and aliquot of the reaction mixture was stored in SDS sample buffer. The remaining trypsinized mGluR113 was cross-linked with EGS and analyzed with the non-cross-linked sample by SDS-PAGE under the reduced condition. The proteolytic fragments, *2* and *4*, were detected in the *lane 2* of trypsinized sample. The cross-linked trypsinized mGluR113 (*lane 4*) was electrophoresed at a position (*asterisk*) similar to that of cross-linked undigested mGluR113 (*lane 3*). These results led us to conclude that the NH_2-terminal 15 kDa fragment was associated with the remaining fragment after trypsin cleavage at Arg-Cys bond after residue 139. Thus, on the basis of the trypsin sensitive site, ^{521}Arg, I designed a new construct, pVLmGluR114, which encodes cDNA corresponding to the region ^{1}Met–^{522}Ser, as shown in *Figure 1*.

Figure 4A shows the immunoblot of the supernatant of the insect (High Five) cells infected with the recombinant viruses for the new shorter soluble receptor protein, mGluR114, as well as for mGluR113. mGluR114 and mGluR113 were detected by

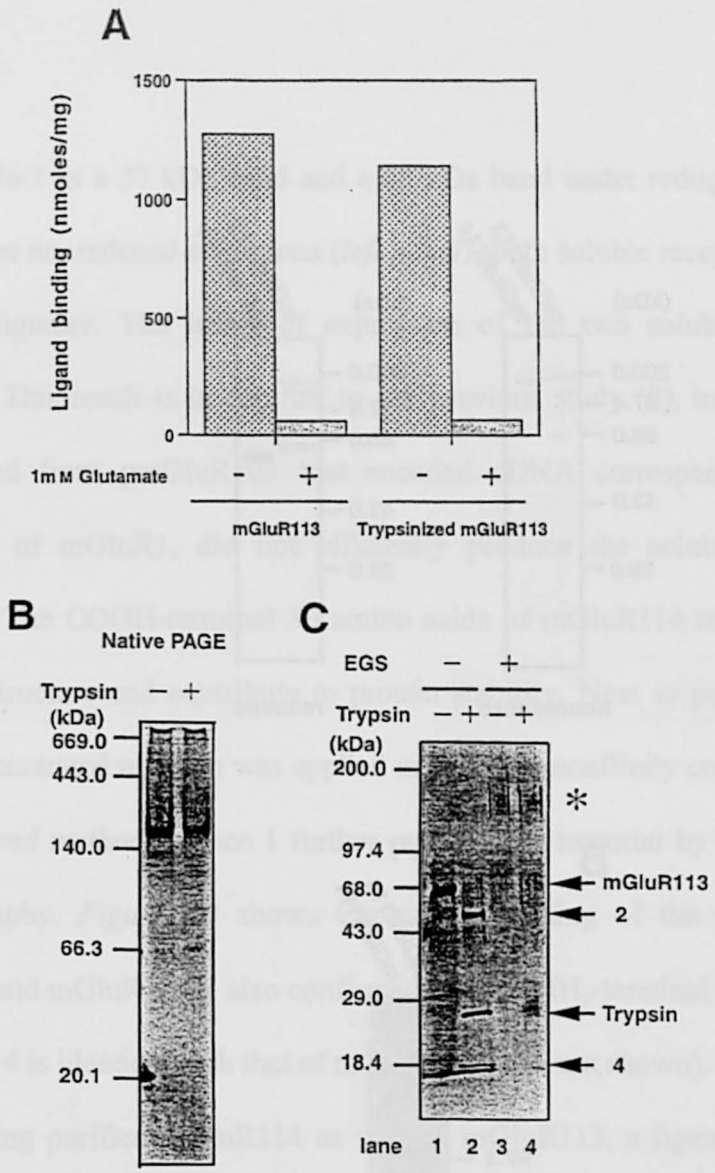

Figure 3. Ligand binding (A), native PAGE analysis (B), and chemical cross-linking (C) of trypsinized mGluR113. *A*, 11.3 μg of mGluR113 purified with an immunoaffinity column was digested with 1.1 μg trypsin at 25 °C for 1 h. After addition of 1 mM PMSF for quench, aliquot containing 0.86 μg of trypsin digested mGluR113 were incubated in the binding buffer (40 mM Hepes, pH 7.5 and 2.5 mM $CaCl_2$) with 20 nM of [^{3}H]quisqualate at 4°C for 1 h. Undigested mGluR113 was assayed as a control. Non-specific binding was measured in the presence of 1 mM glutamate. *B*, trypsin-digested mGluR113 was analyzed by native PAGE. 0.75 μg of mGluR113 purified with an immunoaffinity column was digested with 0.075 μg of trypsin at 25 °C for 1 h. After addition of 1 mM PMSF and sample buffer without SDS, the digested sample was loaded onto a 4–20 % native gradient gel and silver stained. Control sample treated without trypsin was parallelly electrophoresed. *C*, Cross-linking study of trypsinized mGluR113. Immunoaffinity-purified mGluR113 was digested with 10 % (w/w) trypsin at 25 °C for 16 h (*lane 2*). Half of the reaction mixture was cross-linked with 1 mM EGS (*lane 4*). 0.75 μg of protein was loaded on each lane of a 4–20 % SDS gradient gel under reduced conditions. The undigested samples without cross-linking (*lane 1*) and with cross-linking (*lane 3*) underwent with the same procedure parallelly. The asterisk indicates cross-linked material.

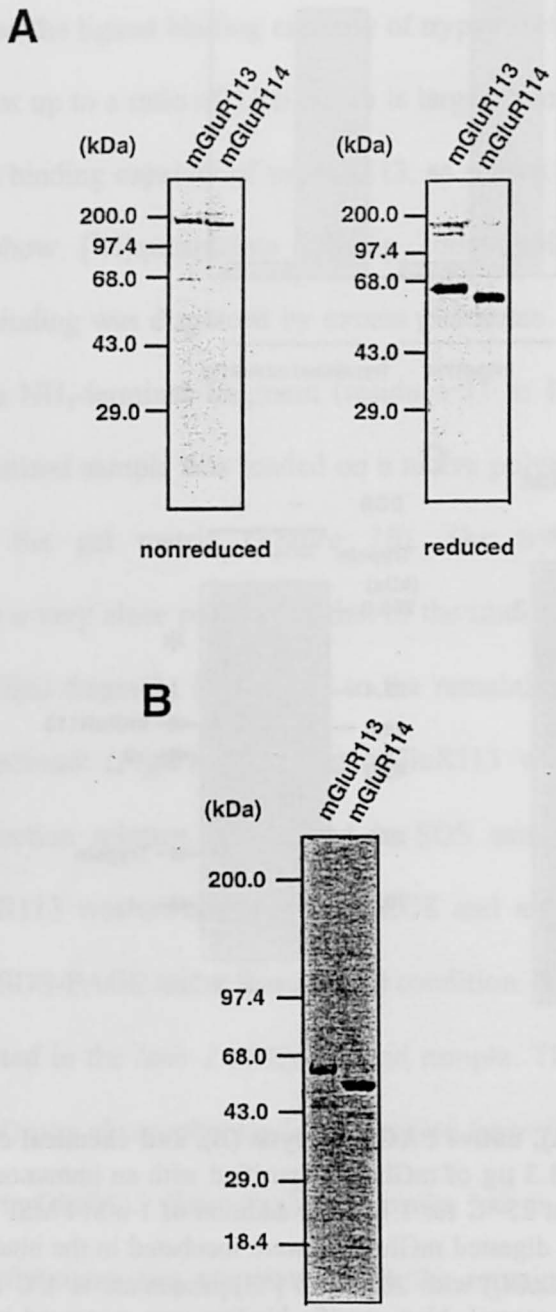

Figure 4. Immunoblotting analysis (A) and Coomassie staining of purified mGluR113 and mGluR114 (B). *A*, 20 µl of culture medium of High Five cells infected with baculoviruses for mGluR113 and mGluR114 were loaded on 10 % SDS-polyacrylamide gels under nonreduced conditions (*left panel*) and reduced conditions (*right panel*). Proteins were transferred onto the nitrocellulose membrane and probed with MAb mG1Na-1. *B*, mGluR113 (4 µg) and mGluR114 (6 µg) purified by Resource Q as described in '*Materials and methods*' were loaded on 10–20 % SDS-polyacrylamide gels and Coomassie stained.

MAb mG1Na-1 as a 57 kDa band and a 65 kDa band under reduced conditions (*right panel*). Under nonreduced conditions (*left panel*), both soluble receptors seemed to be a dimer or oligomer. The levels of expression of the two soluble receptors looked compatible. This result is in contrast to our previous study (8), in which recombinant virus derived from pmGluR103 that encoded cDNA corresponding to the region ^{1}Met–^{492}Glu of mGluR1, did not efficiently produce the soluble receptor protein, mGluR103. The COOH-terminal 30 amino acids of mGluR114 may be involved in a secondary structure and contribute to protein stability. Next to purify mGluR114, the 40-fold concentrated medium was applied on an immunoaffinity column as described in '*Materials and methods*'. Then I further purified the material by Resource Q column chromatography. *Figure 4B* shows Coomassie staining of the purified material of mGluR114 and mGluR113. I also confirmed that the NH_2-terminal amino acid sequence of mGluR114 is identical with that of mGluR113 (data not shown).

Using purified mGluR114 as well as mGluR113, a ligand binding study was performed. mGluR114 and mGluR113 showed saturable binding as in *Figures 5A and 5B* . The K_d value of mGluR114 for quisqualate, which lacks the cysteine-rich region, was 58.1 ± 0.84 nM, similar to the K_d value, 54.1 ± 5.82 nM, of mGluR113. These values are comparable to those reported using full-length membrane bound mGluR1 (17). Thus the LIVBP-like region is sufficient enough to bind ligands. B_{max} values of mGluR 114 and mGluR 113 were 7.06 ± 0.82 nmole/mg protein and 6.92 ± 0.73 nmole/mg protein, respectively. Right panels are Scatchard plots of the data.

In order to obtain insights into the conformational changes that occur upon ligand binding, I performed trypsin digestion of mGluR114 in the presence of a ligand, quisqualate. Tryptic fragments generated by digestion in the presence of quisqualate

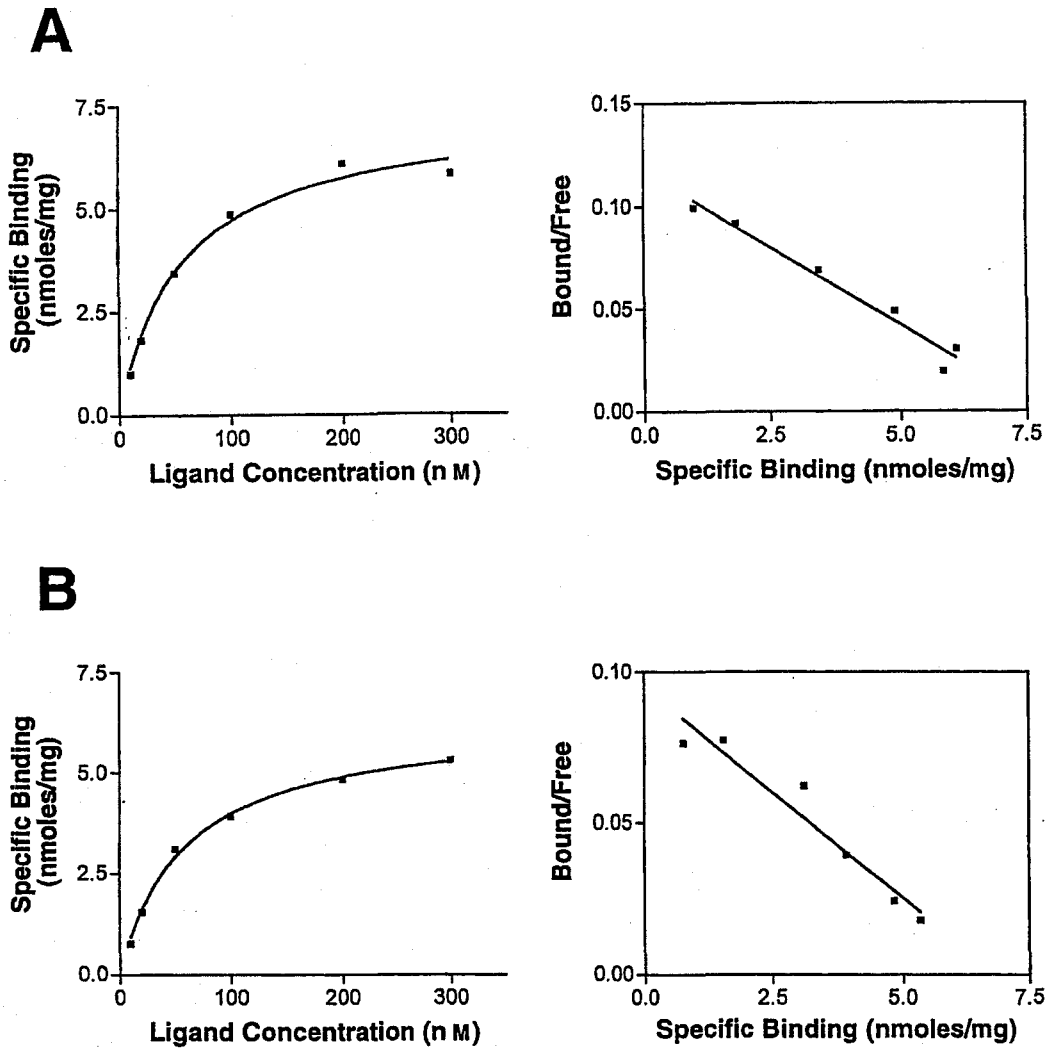

Figure 5. Saturation binding of [^{3}H]quisqualate to mGluR113 and mGluR114. 0.5 μg of immunoaffinity-purified mGluR113 (*A*) and mGluR114 (*B*) were incubated in the binding buffer (40 mM Hepes containing 2.5 mM $CaCl_2$) with different ligand concentrations of [^{3}H]quisqualate at 4 °C for 1 h. Specific binding was determined by subtraction of non-specific binding determined in the presence of 1 mM glutamate from total binding. The results were analyzed by Prism II for saturation kinetics (*left panels*) and for Scatchard analysis (*right panels*). A representative result from three independent experiments is shown. Each binding was performed in triplicate and is shown as the mean ± S.E.M. A non-linear regression analysis of mGluR113 revealed a K_d of 54.1 ± 5.82 nM and a B_{max} of 6.92 ± 0.73 nmoles/mg protein. mGluR114 showed a K_d of 58.1 ± 0.84 nM and a B_{max} of 7.06 ± 0.82 nmoles/mg protein. These K_d and B_{max} values are means ± S.E.M. (n = 3).

apparently differed in protein stability from those generated in the absence of quisqualate. The 40 kDa band, which corresponds to the *fragment 3* in *Figure 2B*, remained when mGluR114 was digested in the presence of quisqualate at a 1/12.5 ratio (*Figure 6*). Furthermore low molecular bands detected between 30 kDa to 21.5 kDa marker proteins appeared to be stable in the presence but not in the absence of the ligand in the lanes of samples digested at the ratio of 1/25 and 1/12.5. Stability of the tryptic fragments appeared to increase in the presence of the ligand. Thus I concluded that trypsin accessibility or sensitivity to mGluR114 was slightly changed by the presence of the ligand.

Next I performed rotary shadowing of the soluble receptor proteins, mGluR114 and mGluR113 (*Figure 7*). Both were globular proteins consisting of two similar components facing each other, consistent with the above finding that they were electrophoresed as dimers in the native gels. Remarkable difference in the shadowing image was not observed between mGluR114 and 113, implying that the LIVBP-like region can fold regardless of the presence or absence of the cysteine-rich region.

Discussion

I have succeeded in outlining the domain structure of the extracellular region of mGluR1. A number of Arg and Lys residues are distributed in the extracellular region, nevertheless, trypsin digested mGluR113, which consists of the whole extracellular region of mGluR1, at the site of ^{521}Arg. Thus the extracellular region of mGluR1 was subdivided into two domains: an NH_2-terminal LIVBP-like region and a cysteine-rich region preceding the first transmembrane segment. I call the former part the ligand binding domain (LBD) and the latter the cysteine-rich domain (CRD) hereafter.

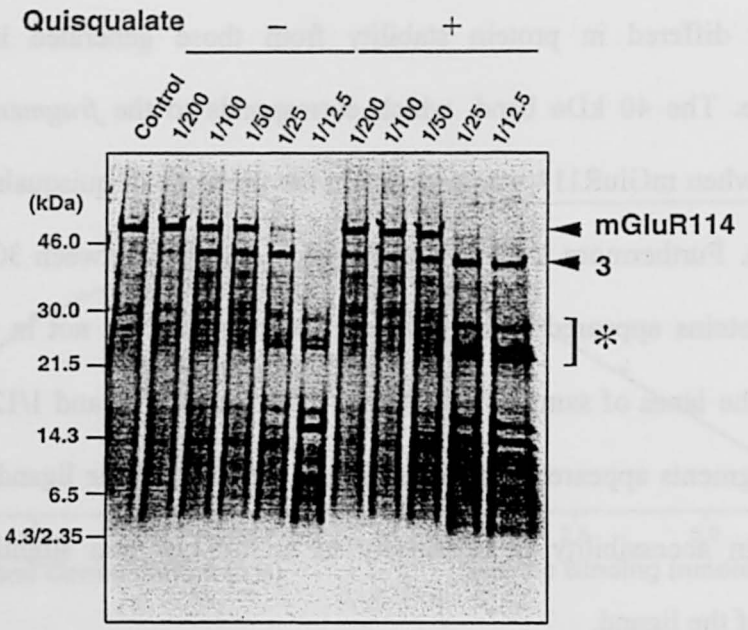

Figure 6. Limited proteolysis of mGluR114 in the presence and absence of ligand. mGluR114 purified with an immunoaffinity column was incubated with and without 1 mM quisqualate for 15 min in 10 mM Hepes, pH 7.5. Aliquots (12 µg protein) were digested with trypsin at the indicated ratios (w/w) at 25 °C for 1 h and were loaded on a 15–25 % SDS polyacrylamide gel. Untreated mGluR114 was electrophoresed as a control. The gel was silver stained.

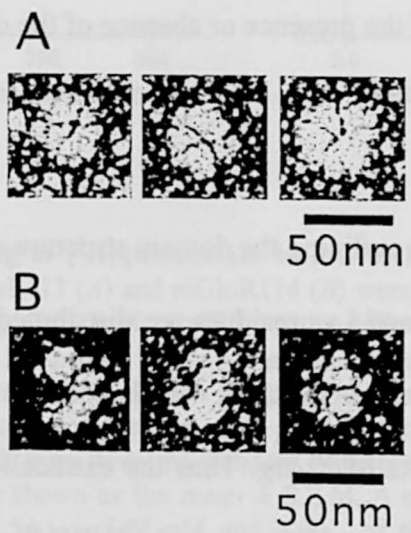

Figure 7. Rotary shadowing image of the soluble mGluRs. Gallery of electron micrographs of soluble mGluR113 (A) and mGluR114 (B).

Furthermore five major fragments generated by partial tryptic digestion was assigned according to the two trypsin sites.

An extracellular fragment devoid of CRD, mGluR114, was expressed well and showed a K_d value of 58.1 ± 0.84 nM for its ligand, [^{3}H]quisqualate, which is close to that of mGluR113. Both of the soluble receptors, mGluR113 and mGluR 114, showed dimer under nonreduced conditions and monomer under reduced conditions. Thus cysteine residue(s) responsible for the intermolecular disulfide bond reside within LBD. We have identified the cysteine residue that forms the intermolecular disulfide bond within LBD (18). Because the trypsin-digested mGluR113 electrophoresed at a position similar to that of the undigested one under a native condition, nick introduced by trypsin treatment seems not to interfere with the dimer interface. Interestingly, trypsin-digested mGluR113 as well as mGluR114 (data not shown) retains ligand binding activity, suggesting that the digestion site, ^{139}Arg, is exposed to the surface and resides in a flexible region. The NH_2-terminal 15 kDa fragment seems to be associated with the remaining part after trypsin digestion. Therefore I did not make an expression construct that did not contain the corresponding cDNA sequence. Thus whether the 15 kDa fragment is required for ligand binding could not be determined. The 15 kDa region might have a role for folding LBD. I speculate that the ligand binding site forms a rather rigid structure.

A slight difference was observed in trypsin accessibility to mGluR114 between the presence of ligand and the absence of it. The effect of ligand on stability of proteolytic fragment of a soluble form of GluR2, a member of ionotropic glutamate receptor, has been studied by Chen *et al.* (19). They showed that a main proteolytic fragment was more stable in the presence of ligand during trypsin digestion. They

compared trypsin sensitivity of the purified soluble receptors that differ in the flanking sequences with and without the ligands, and found a stable construct which is resistant to trypsin and suitable for structural study.

Provided that two molecules of the ligand, quisqualate, bind to a dimer form of the soluble receptor, the stoichiometry of binding can be calculated to be approximately 39–44 % based on the B_{max} values of mGluR113 and mGluR114 for the ligand. Only half of the material might retain binding capacity. Or I may have been unable to measure maximal binding capacity because our PEG precipitation assay is not expected to resolve low affinity site, if any, with a K_d in the micromolar range. However, if I assume that cooperative binding is operated in the dimer form of the mGluR1 or the two binding sites possess different affinities, this value of stoichiometry would be meaningful. Interestingly, it has been reported that a purified 42 kDa ligand-binding fragment of GluR-D, an α-amino-3-hydroxy-5-methyl-4-isoxazolepropionic acid receptor, one of glutamate-gated ion channels, showed a B_{max} value of 6–12 nmol/mg, indicating 50 % stoichiometry of the theoretical maximum (20).

Whether or not CRD interacts with LBD or the transmembrane region is still unknown. The absence of large differences between the rotary shadowing image of mGluR113 and mGluR114 suggests that CRD appears not to perform major roles in dimer formation. Ligand binding within LBD may elicit conformational change of the seven transmembrane segments through CRD. If the structure of CRD is not flexible, magnitude and orientation of the conformational change occurred within LBD, if any, would transmit directly to the seven transmembrane helices. Or CRD may be a flexible stalk and remold itself upon ligand binding to LBD. Thus elucidation of the structure and function of CRD is an intriguing challenge. Through structural analysis of the

ligand binding core of GluR2, Armstrong *et al.* pointed out a possible interacting site to the allosteric effector or of domain-domain contact through its hydrophobic character (21). CRD in mGluR might be involved in such an interaction, although I do not have any evidence.

Recently dimer formation has been reported in several G-protein coupled receptors such as dopamine receptors and opioid receptors. Although the significance of dimer formation in ligand binding or signal transmission of GPCRs has not been extensively explored, it is reported that κ-δ opioid receptor heterodimer acquired an affinity and selectivity different to those of the two functional opioid receptors, κ and δ (22). Thus the possibility of heterodimerization among the eight subtypes of mGluRs should be carefully examined.

Because of the nine cysteine residues in a 70 amino-acid stretch, mGluR113 preparation might contain some misfolded material. Thus mGluR114 complexed with ligands may be a good candidate for use in analysis of the tertiary structure of mGluR1.

Acknowledgments

I thank Dr. Yutaka Takeuchi for [^{3}H]quisqualate. I am grateful to Dr. Yoshiro Shimura for continuous encouragement and suggestions.

References

1. Masu, M., Tanabe, Y., Tsuchida, K., Shigemoto, R., and Nakanishi, S. (1991) *Nature* **349,** 760–765.
2. Nakanishi, S., and Masu, M. (1994) *Annu. Rev. Biophys. Biomol. Struct.* **23,** 319–348.

3. O'Hara, P. J., Sheppard, P. O., Thøgersen, H., Venezia, D., Haldeman, B. A., McGrane, V., Houamed, K. M., Thomsen, C., Gilbert, T. L., and Mulvihill, E. R. (1993) *Neuron* **11,** 41–52.

4. Kaupmann, K., Huggel, K., Heid, J., Flor, P. J., Bischoff S., Mickel S. J., McMaster, G., Angst, C., Bittiger, H., Froestl, W., and Bettler, B. (1997) *Nature* **386,** 239–246.

5. Herrada, G., and Dulac, C. (1997) *Cell* **90,** 763–773.

6. Matsunami, H., and Buck, L. B. (1997) *Cell* **90,** 775–784.

7. Brown, E. M., Gamba, G., Riccardi, D., Lombardi, M., Butters, R., Kifor, O., Sun, A., Hediger, M. A., Lytton, J., and Hebert, S. C. (1993) *Nature* **366,** 575–580.

8. Okamoto, T., Sekiyama, N., Otsu, M., Shimada, Y., Sato, A., Nakanishi, S., and Jingami, H. (1998) *J. Biol. Chem.* **273,** 13089–13096.

9. Romano, C., Yang, W. L., and O'Malley, K. L. (1996) *J. Biol. Chem.* **271,** 28612–28616.

10. Han, G., and Hampson, D. R. (1999) *J. Biol. Chem.* **274,** 10008–10013.

11. Bai, M., Trivedi, S., and Brown, E. M. (1998) *J. Biol. Chem.* **273,** 23605–23610.

12. Goldsmith, P. K., Fan, G. F., Ray, K., Shiloach, J., McPhie, P., Rogers, K. V., and Spiegel, A. M. (1999) *J. Biol. Chem.* **274,** 11303–11309.

13. Quiocho, F. A. (1990) *Philos. Trans. R. Soc. Lond. B Biol. Sci.* **326,** 341–351.

14. Neki, A., Ohishi, H., Kaneko, T., Shigemoto, R., Nakanishi, S., and Mizuno, N. (1996) *Neurosci. Lett.* **202,** 197–200.

15. Shigemoto, R., Kinoshita, A., Wada, E., Nomura, S., Ohishi, H., Takada, M.,

Flor, P. J., Neki, A., Abe, T., Nakanishi, S., and Mizuno, N. (1997) *J. Neurosci.* **17,** 7503–7522.

16. Miyazaki, J., Nakanishi, S., and Jingami, H. (1999) *Biochem. J.* **340,** 687–692.

17. Ohashi, H., Higashi-Matsumoto, H., Maruyama, T., and Takeuchi, Y. (1997) *Soc. Neurosci. Abstr.* **23,** 2023.

18. Tsuji, Y., Shimada Y., Takeshita T., Kajimura N., Nomura S., Sekiyama N., Otomo J., Usukura J., Nakanishi S., and Jingami H. (2000) *J. Biol. Chem.* **275,** 28144–28151.

19. Chen, G. Q., Sun, Y., Jin, R., and Gouaux, E. (1998) *Protein Sci.* **7,** 2623–2630.

20. Kuusinen, A., Arvola, M., and Keinänen, K. (1995) *EMBO J.* **14,** 6327–6332.

21. Armstrong, N., Sun, Y., Chen, G. Q., and Gouaux, E. (1998) *Nature* **395,** 913–917.

22. Jordan, B. A., and Devi, L. A. (1999) *Nature* **399,** 697–700.

CONCLUSIONS

CHAPTER I

SECTION I

Previously it was determined that an Arg-Gly-Asp (RGD)-inserted mutant between ^{74}Val and ^{75}Asn of human lysozyme named 74RGD4 had relatively high cell adhesion activity as well as full lytic activity. To increase the cell adhesion activity of 74RGD4, another RGD sequence was engineered into lysozyme. I found that 47RGD4 with RGDS in place of AGDR (residues 47 to 50) in a β-turn region possesses the same level of adhesion activity as that of 74RGD4. The acceptance of the RGD introduction in the β-turn region of human lysozyme is in good agreement with recent studies on the functional conformation of RGD. I constructed (47,74)RGD4, a mutant containing RGD at two sites, by combining the NH_2-terminal domain of 47RGD4 and the COOH-terminal domain of 74RGD4. The (47,74)RGD4 lysozyme, with two functional RGD sequences, exhibits even higher cell adhesion activity than that of 74RGD4 or 47RGD4. The two RGD introduction sites of (47,74)RGD are located at a considerable distance (19.4 Å). Thus the (47,74)RGD4 mutant may be useful as a functional cross-linker in RGD dependent cell-to-cell interactions, differently from 74RGD4 or 47RGD4.

SECTION II

To tailor tissue-type plasminogen activator (tPA) to possess an affinity for the integrins, I introduced the RGD sequence individually into the tPA molecule at several locations. These mutants were expressed in COS-1 cells and partially purified by lysine-Sepharose chromatography. The RGD-dependent binding of the mutants to platelet integrin, integrin $\alpha_{IIb}\beta_3$, was evaluated by subtracting the non-specific binding in the

presence of 10 mM EDTA (or 1 mg/ml GRGDSP). The binding assay showed that two tPA mutants possess high affinity for the integrin in an RGD-dependent manner. One mutant is 148RGD-tPA with RGDS in place of DRDS (residues 148 to 151) in the loop region of the kringle 1 domain of tPA, and the other is 270 RGD-tPA with RGDS in place of SQPQ (residues 270 to 273) in the linker region of the kringle 2 and protease domains. Using the chromogenic substrate Spectrozyme tPA, the 148RGD-tPA mutant was shown to possess amidolytic activity comparable with that of native tPA, while the 270RGD-tPA mutant exhibited several-fold lower activity. In addition, the 148RGD-tPA exhibited full tPA activity even when interacting with the integrin $\alpha_{IIb}\beta_3$. These results suggest that the bi-functional 148RGD-tPA molecule might be useful as an improved thrombolytic agent specific for the platelet integrin $\alpha_{IIb}\beta_3$.

CHAPTER II

Previously the whole extracellular region of metabotropic glutamate receptor subtype 1 (mGluR1) was produced in a soluble form by the baculovirus/insect cell system. The purified receptor protein retained a ligand affinity comparable with that of the full-length membrane-bound receptor and formed a disulfide-linked dimer. However, the domain organization of the extracellular region of mGluR1 was less clear. In this study, I determined the NH_2-terminal amino acid sequence of the purified whole extracellular fragment and found that the amino acid sequence of the soluble receptor protein began with a residue ^{33}Ser. I have then performed limited proteolysis of the purified whole extracellular fragment (residues 33 to 592) and found two trypsin sensitive sites, after the residues ^{139}Arg and ^{521}Arg. A 15 kDa NH_2-terminal proteolytic fragment (residues 33 to 139) was still associated the rest of the protein after the

digestion. The second site, ^{521}Arg, was located just before a cysteine-rich stretch preceding the transmembrane region. Thus, on the basis of the protease sensitive boundary, a new shorter soluble receptor (residues 33 to 522), which was devoid of the cysteine-rich region, was designed. This receptor protein was well expressed in the baculovirus/insect cell system and showed a ligand-binding capability for [^{3}H]quisqualate. I purified the soluble receptor protein and obtained a K_d value of 58.1 ± 0.84 nM, which is comparable to a reported K_d value of 52.6 nM, of the full-length receptor. The B_{max} value was 7.06 ± 0.82 nmole/mg protein, indicating 40 % of the theoretical maximum calculated on the assumption that the ligand binds to the receptor at 2:2 stoichiometry. These results indicated that the ligand-binding specificity of mGluR1 is confined to the NH_2-terminal 490 amino acid region of the mature protein.

ACKNOWLEDGMENTS

This study has been carried out in Protein Engineering Research Institute (PERI) for CHAPTER I and in Biomolecular Engineering Research Institute (BERI) for CHAPTER II.

I wish to express my sincere gratitude to Dr. Hidehiko Kumagai, Professor of Kyoto University, for his heartwarming encouragement and helpful advice to complete this thesis.

I am thankful to Dr. Masakazu Kikuchi, Professor of Ritsumeikan University, for kindly acceptance to his project in PERI when my starting this course of study. I am grateful to Dr. Takao Yamada from Takeda Chemical Industries, Ltd. for his generous guidance. I also thank to Dr. Atsuko Uyeda of Osaka National Research Institute, AIST., for her encouraging comment.

I am deeply grateful to Dr. Hisato Jingami,Research Directorof Department of Molecular Biology in BERI, who really introduced me into science. I also thank to Mr. Yuji Tsuji from Toyobo Co., Ltd. for his kind collaboration.

I also wish to appreciate his sympathetic encouragement of Dr. Kenji Yamamoto, Professor of Kyoto University.

Last but not least, I extend my thanks to the best partner in my life, Dr. Hisashi Ashida, for his helpful suggestions.

Yoshimi Shimada

Yoshimi Shimada

LIST OF PUBLICATIONS

CHAPTER I

SECTION I

1. Yamada, T., Shimada, Y., Uyeda, A., Sugiyama, S., and Kikuchi, M. (1995) Construction of a divalent cell adhesive lysozyme by introducing the Arg-Gly-Asp sequence at two sites. *FEBS lett.* **374**, 262–264.

SECTION II

1. Yamada, T., Shimada, Y., and Kikuchi, M. (1996) Integrin-specific tissue-type plasminogen activator engineered by introduction of the Arg-Gly-Asp sequence. *Biochem. Biophys. Res. Commun.* **228**, 306–311.

CHAPTER II

1. Tsuji, Y., Shimada, Y., Takeshita, T., Kajimura, N., Nomura, S., Sekiyama, N., Otomo, J., Usukura, J., Nakanishi, S., and Jingami, H. (2000) Cryptic dimer interface and domain organization of the extracellular region of metabotropic glutamate receptor subtype 1. *J. Biol. Chem.* **275**, 28144-28151.

OTHERS

1. Tamaki, H., Kumagai, H., Shimada, Y., Kashima, T., Obata, H., Kim, C. S., Ueno, T., and Tochikura, T. (1991) Detoxification metabolism of *o*-dinitrobenzene by yeast *Issatochenkia orientalis*. *Agric. Biol. Chem.* **55**, 951–956.
2. Takeuchi, M., Kawai, F., Shimada, Y., and Yokota, A. (1993) Taxonomic study

of polyethylene glycol-utilizing bacteria: Emended description of the genus *Sphingomonas* and new description of *Sphingomonas macrogoltabidus* sp. nov., *Sphingomonas sanguis* sp. nov., *Sphingomonas terrae* sp. nov. *Sys. Appl. Microbiol.* **16**, 227–238.

3. Yamada, T., Song, H., Inaka, K., Shimada, Y.. Kikuchi, M., and Matsushima, M. (1995) Structure of a conformationally constrained Arg-Gly-Asp sequence inserted into human lysozyme. *J. Biol. Chem.* **270**, 5687–5690.

4. Okamoto, T., Sekiyama, N., Otsu, M., Shimada, Y., Sato, A., Nakanishi, S., and Jingami, H. (1998) Expression and purification of the extracellular ligand binding region of metabotropic glutamate receptor subtype 1. *J. Biol. Chem.* **273**, 13089–13096.

5. Sato, A., Shimada, Y., Herz, J., Yamamoto, T., and Jingami, H. (1999) 39-kDa receptor associated protein (RAP) facilitates secretion and ligand binding of extracellular region of very-low-density-lipoprotein receptor. *Biochem. J.* **341**, 377–383.

6. Kunishima N., Shimada Y., Tsuji Y., Sato T., Yamamoto M., Kumasaka T., Nakanishi S., Jingami H. and Morikawa K. (2000) Structural basis of glutamate recognition by a dimeric metabotropic glutamate receptor. *Nature.* **407**, 971-977.